ELSEVIER

NeuroImage

www.elsevier.com/locate/ynimg
NeuroImage 29 (2006) 764 – 773

Localizing human visual gamma-band activity in frequency, time and space

Nienke Hoogenboom,[a,b,*] Jan-Mathijs Schoffelen,[a,b] Robert Oostenveld,[a,c] Laura M. Parkes,[a] and Pascal Fries[a,b]

[a]*F.C. Donders Centre for Cognitive Neuroimaging, Radboud University Nijmegen, 6525 EN Nijmegen, The Netherlands*
[b]*Department of Biophysics, Radboud University Nijmegen, 6525 EZ Nijmegen, The Netherlands*
[c]*Center for Sensory-Motor Interaction (SMI), Aalborg University, Fredrik Bajers Vej 7 D-3, 9220 Aalborg, Denmark*

Received 20 January 2005; revised 17 June 2005; accepted 23 August 2005
Available online 10 October 2005

Neuronal gamma-band (30–100 Hz) synchronization subserves fundamental functions in neuronal processing. However, different experimental approaches differ widely in their success in finding gamma-band activity. We aimed at linking animal and human studies of gamma-band activity and at preparing optimized methods for an in-depth investigation of the mechanisms and functions of gamma-band activity and gamma-band coherence in humans. In the first step described here, we maximized the signal-to-noise ratio with which we can observe visually induced gamma-band activity in human magnetoencephalographic recordings. We used a stimulus and task design that evoked strong gamma-band activity in animals and combined it with multi-taper methods for spectral analysis and adaptive spatial filtering for source analysis. With this approach, we found human visual gamma-band activity very reliably across subjects and across multiple recording sessions of a given subject. While increases in gamma-band activity are typically accompanied by decreases in alpha- and beta-band activity, the gamma-band enhancement was often the spectral component with the highest signal-to-noise ratio. Furthermore, some subjects demonstrated two clearly separate visually induced gamma bands, one around 40 Hz and another between 70 and 80 Hz. Gamma-band activity was sustained for the entire stimulation period, which was up to 3 s. The sources of gamma-band activity were in the calcarine sulcus in all subjects. The results localize human visual gamma-band activity in frequency, time and space and the described methods allow its further investigation with great sensitivity.

Introduction

Increasing evidence suggests that neuronal gamma-band (30–100 Hz) synchronization is a fundamental process involved in several important brain functions, including visual feature binding (Eckhorn et al., 1988; Gray et al., 1989; Tallon-Baudry et al., 1996; Mima et al., 2001), perceptual and attentional stimulus selection (Steinmetz et al., 2000; Fries et al., 2001, 2002), visuomotor control (Bressler et al., 1993; Roelfsema et al., 1997; Rodriguez et al., 1999), working memory (Tallon-Baudry et al., 1998; Lutzenberger et al., 2002; Pesaran et al., 2002) and associative learning (Miltner et al., 1999). Most of the early evidence for a functional role of neuronal gamma-band synchronization came from recordings in the visual cortex of anesthetized, paralyzed cats (Eckhorn et al., 1988; Gray and Singer, 1989; Gray et al., 1989, 1992; Engel et al., 1991). This was followed by recordings in visual cortex of awake, trained monkeys (Kreiter and Singer, 1996; Gail et al., 2000; Fries et al., 2001). Those invasive microelectrode recordings of spikes and local field potentials typically demonstrated gamma-band activity with very high signal-to-noise ratio. Conversely, electroencephalographic (EEG) and magnetoencephalographic (MEG) recordings in humans often show only marginally small fluctuations in the gamma band. It was only within the last decade that the interest in the study of gamma-band activity with EEG and MEG in humans increased strongly. In the meantime, numerous studies have demonstrated the existence of gamma-band activity in the human brain and its modulation by, for example, perceptual organization (Tallon-Baudry et al., 1996, 1997a; Keil et al., 1999), attention (Gruber et al., 1999), working memory (Tallon-Baudry et al., 1998; Lutzenberger et al., 2002; Kaiser et al., 2003) and associative memory (Miltner et al., 1999; Gruber et al., 2001). Despite this growing interest, gamma-band activity has remained elusive. Some groups reported difficulties in finding any gamma-band activity that is not phase-locked to stimulus onset. Furthermore, it appeared particularly difficult to demonstrate gamma-band activity with MEG. Some studies failed to find induced gamma-band

* Corresponding author. F.C. Donders Centre for Cognitive Neuroimaging, Radboud University Nijmegen, 6525 EN Nijmegen, The Netherlands. Fax: +31 24 36 10989.
E-mail address: n.hoogenboom@fcdonders.ru.nl (N. Hoogenboom).
Available online on ScienceDirect (www.sciencedirect.com).

1053-8119/$ - see front matter © 2005 Elsevier Inc. All rights reserved.
doi:10.1016/j.neuroimage.2005.08.043

activity in the MEG (Tallon-Baudry et al., 1997b). Other MEG studies succeeded in demonstrating significant experimental effects in narrow frequency ranges within the gamma band, but effect sizes were small (Lutzenberger et al., 2002; Kaiser et al., 2003). Only very recently did one MEG study describe strong, sustained gamma-band activity induced by a visual illusion and located it to early visual cortex (Adjamian et al., 2004).

We set out to adopt a stimulus and task design from monkey experiments that has proven to induce strong visual cortical gamma-band activity and to optimize data analysis procedures to demonstrate visually induced gamma-band activity both at the sensor and at the source level. The methods described here constitute a window onto human visual gamma-band activity that can be used for further analysis of its functional role in human cognition.

Materials and methods

Subjects

Seven right-handed subjects (four male, three female; mean age 23, range 17–26), without any known history of neurological disorders participated in the study. All had normal or corrected-to-normal visual acuity. Before the experiment, informed consent was obtained from each subject according to the Declaration of Helsinki. One subject was 17 years of age when participating in the study and therefore parental consent was obtained.

Experimental paradigm and stimuli

The experimental paradigm and the stimuli are illustrated in Fig. 1. Each trial started with the presentation of a fixation point (Gaussian of diameter 0.5°). After 500 ms, the fixation point contrast was reduced by 40%, which served as a warning. After another 1500 ms, the fixation point was replaced by a foveal, circular sine wave grating (diameter: 5°; spatial frequency: 2 cycles/deg; contrast: 100%). The sine wave grating contracted toward the fixation point (velocity: 1.6 deg/s) and this contraction accelerated (velocity step to 2.2 deg/s) at an unpredictable moment between 50 and 3000 ms after stimulus onset. The subjects' task was to press a button with their right index finger within 500 ms of this acceleration. 10% of the trials were catch trials in which no acceleration occurred. The stimulus was turned off after a response was given, or in catch trials 3000 ms after stimulus onset. Stimulus offset was followed by a resting period of 1000 ms in which subjects were given visual feedback about the correctness of their response and were asked to blink. Stimuli were presented using an LCD projector located outside the magnetically shielded room of the MEG (see below) and back-projected onto a translucent screen via two front-silvered mirrors. The vertical refresh rate of the LCD-projector was 60 Hz. Control measurements with a sensitive photodiode showed no 60-Hz component in the luminance time course of the stimuli. Each subject completed six blocks of 75 trials. At the end of each block, visual feedback was given about the percentage correct responses and the upcoming block number. A typical recording session lasted about 50 min. All stimuli were presented using the 'Presentation' software package (Neurobehavioral Systems, Inc.).

Three out of seven subjects (1 male, 2 female) also participated in a functional magnetic resonance imaging (fMRI) experiment using identical stimuli, but extending the baseline period to 10,000 ms. fMRI trials were grouped in three blocks of 50 trials.

Data acquisition

MEG signals were recorded using a 151-sensor whole head system (CTF systems Inc., Port Coquitlam, Canada). The simultaneously recorded electrooculogram (EOG) was used for offline artifact rejection. The data were low-pass filtered at 300 Hz and digitized at 1200 Hz. Prior to and after the MEG recording, the subject's head position relative to the gradiometer array was determined using coils positioned at the subject's nasion, and at the left and right ear canal.

Structural and functional magnetic resonance images were obtained using a 1.5-T (all structural MRIs and the fMRIs of subjects A and B) and a 3-T (fMRIs of subject C) whole body MRI scanner (Siemens, Erlangen, Germany). A volume head coil was used for RF transmission and signal reception. Functional images were acquired using a gradient-echo EPI sequence (TR 2000 ms, TE 40 ms, band width 1860 Hz, flip angle 80°) with 25 slices (224 mm FOV, 64 × 64 matrix, 3.5 mm thickness, 0.35 mm gap) covering all cortical structures. This gives a standard blood oxygenation level-dependent (BOLD) response. A 3D MPRAGE sequence with 1 mm isotropic resolution was used for the structural scan.

MEG-data analysis

All MEG data analysis was done in the Fieldtrip open source Matlab toolbox (http://www.ru.nl/fcdonders/fieldtrip/) that was developed at the F.C. Donders Centre for Cognitive Neuroimaging. Three main analyses were done: an analysis of the overall effect of visual stimulation on the power-spectra at the sensor level, an analysis of the time course of power at the sensor level and an analysis of the sources underlying the different spectral components.

All three analyses started with the same preprocessing steps: Data epochs of interest were defined as such from the continuously recorded MEG. Data epochs that were contaminated by eye movements, muscle activity or jump artifacts in the SQUIDs were discarded using semi-automatic artifact rejection routines. The

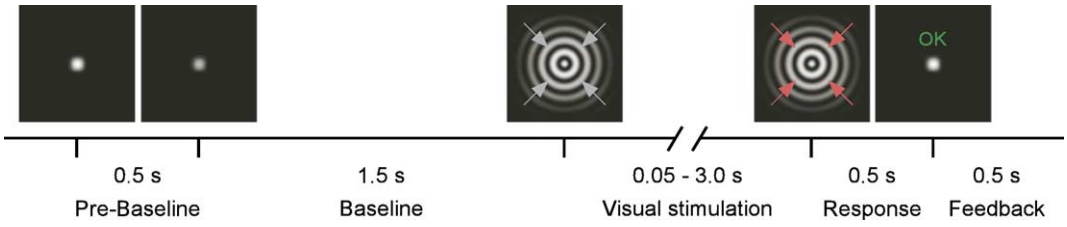

Fig. 1. The experimental paradigm.

power line fluctuations were removed by estimating and subtracting the 50-, 100- and 150-Hz components in the MEG data, using a discrete Fourier transform (DFT) on 10-s data segments surrounding the data epochs of interest. The data epochs of interest were then cut out of these cleaned 10-s segments and the linear trend was removed from each epoch.

Spectral analysis at the sensor level

For the analysis of the overall effect of visual processing on oscillatory neuronal synchronization, we compared the power spectra of the MEG data epochs in the stimulus condition with those in the baseline condition. The stimulus condition contained all data until the moment of the speed change but excluded the first 500 ms after stimulus onset to discard response onset transients. Epochs in the baseline condition extended from 1000 ms before stimulus onset until stimulus onset. Data epochs from both conditions were considered separately in further analyses. Each epoch was tapered using discrete prolate spheroidal sequences (Slepian functions) (Mitra and Pesaran, 1999). This multi-taper method was used to improve the consecutive spectral estimation. Because the resulting tapered data epochs had a variable duration across trials, they were first zero-padded to a length of 4 s and then Fourier transformed. Average spectral power was then computed as the average across trials and tapers. The tapering used in this analysis yielded a spectral concentration of ±1 Hz around each center frequency. For a first assessment of the effect of visual processing, we analyzed spectral power of 28 parietooccipital MEG sensors (LP11, LP12, LP21, LP22, LP31, LP32, LO11, LO12, LO21, LO22, LO31, LO32, RP11, RP12, RP21, RP22, RP31, RP32, RO11, RO12, RO21, RO22, RO31, RO32, ZP01, ZP02, ZO01, ZO02). The power estimates were averaged across sensors, and we obtained a variance estimate for the spectral power by applying a jackknife procedure (Efron and Tibshirani, 1993). Subsequently, a frequency-wise t value was determined (Press et al., 1992) between the period of sustained visual activation and the baseline period.

Time course analysis at the sensor level

For the analysis of the time courses of the power, time frequency representations (TFRs) were computed using a short-time discrete Fourier transform on 400-ms data epochs sliding in 50-ms steps. For this analysis, we used the same parietooccipital sensors that were used for the first analysis step, and data from 1400 ms before stimulus onset until 2300 ms after stimulus onset. All frequencies between 5 and 120 Hz in steps of 2.5 Hz were considered. A spectral smoothing of ±5 Hz around each center frequency was obtained using multi-tapering. The TFRs were expressed as a percent change with respect to the baseline (1000 ms period before stimulus onset).

Spectral component analysis at the source level

For the analysis of the neuronal sources of the different spectral components, we used an adaptive spatial filtering technique (Gross et al., 2001). Each subject's brain volume was divided into a regular 5-mm grid and for each grid location, a spatial filter was constructed. This filter has the property that it optimally passes activity from the location of interest while activity from all other brain regions is optimally suppressed. It is calculated by taking into account the forward model at the location of interest (the leadfield matrix) and the cross-spectral density between all MEG signal pairs at the frequency of interest. To compute the leadfield matrix, we used a multisphere model in which, for each sensor, a sphere was fitted to the head surface underlying that sensor. The head shape was derived from each individual subject's structural MRI and aligned to the MEG data.

We inspected the percent change spectra and determined clearly separated peaks or troughs by eye for each individual subject. The cross-spectral density between all MEG sensor pairs at the frequencies of interest was computed for all trials, separately for all epochs in the baseline and visual stimulation condition. To minimize the variance in the estimate of the cross-spectral densities, multi-tapering was adjusted per subject and frequency band to include an optimized spectral concentration around each center frequency.

Consecutively, spatial filters were constructed for each grid location and separately for the baseline and the visual stimulation condition and the data of each condition was projected through the respective filters. This resulted in an estimate of the source power for the visual stimulation and baseline period, based on the cross-spectral density averaged over all stimulation and baseline epochs, respectively.

To quantify the effect of visual stimulation on the oscillatory activity, we computed a voxel-wise t value. The variance in the power at each voxel was estimated using a jackknife procedure. For each condition, the source distribution was recomputed N times, leaving out one trial each time for the construction of, and the projection through the spatial filters.

A statistical interpretation of the resulting volumetric t values is not straightforward because of the large number of voxels to be tested and because the estimated source power is not necessarily normally distributed. Therefore, to identify source locations that were significantly modulated by visual stimulation, we adopted a non-parametric randomization approach (Nichols and Holmes, 2001). This procedure does not rely on an underlying distribution, and it allows for a solution to the multiple comparisons problem. The null hypothesis states that there is no difference between the cross-spectral density for the two conditions, and hence also no difference in the estimated source parameters. Therefore, a random rearrangement of the data over the two conditions, followed by a source reconstruction of the data in both conditions, results in the difference in the estimated source parameter at each voxel that is equally likely under the null hypothesis. Instead of taking the difference at each voxel separately as the test statistic, we selected the voxel with the largest difference over the whole volume. An estimate of the null distribution of this maximum difference statistic is obtained by repeating this for a large number of randomizations. At each grid location, the observed difference is then tested against the distribution of our test statistic, yielding the probability of observing that difference under the null hypothesis. Since our test statistic consists of the maximum difference over the whole volume, we are controlling for the false alarm rate.

We performed the following steps 500 times: The multi-tapered cross-spectral densities were computed for all epochs in the stimulus (S) and baseline (B) condition and were randomly reassigned to an S* and a B* condition, such that the number of trials in conditions S* and S was equal as well as in conditions B* and B. Two sets of spatial filters were constructed using the averaged cross-spectral density of the respective randomly reassigned conditions S* and B*. The randomly reassigned data were

then projected through these filters, and the resulting source reconstruction of condition B* was subtracted from the source reconstruction of condition S*.

A feature of the spatial filtering method is that noise in the data tends to project to deeper source locations. Hence, the spatial distribution of the projected noise is not homogenous. The distribution of the difference was normalized by computing the *Z*-transform of the difference in the estimated source power across all randomizations for each voxel separately. The reference distribution was then obtained by taking from each randomized difference volume, the maximal *Z*-transformed value. This procedure directly corrects for the multiple comparisons done on all grid locations. The *Z*-transformed difference value at each grid location in the observed data was tested against this reference distribution, and the probability of observing that value under the null hypothesis was computed.

fMRI data analysis

The fMRI data were processed using the BrainVoyager software package (BrainVoyager 2000, Brain Innovation, Maastricht, The Netherlands). The first three images (6 s) of each functional data set were discarded to allow time for the longitudinal magnetization of the water protons to reach equilibrium. The data were preprocessed using motion correction, a correction for the different slice timings, linear trend removal to remove baseline drifts and a high pass filter of 0.006 Hz to remove very slow fluctuations in the BOLD signal time course. For two subjects, the functional data were aligned to the anatomical scan that was made during the fMRI session. For the third subject, the anatomical and functional scans were acquired in different sessions and manual adjustment was necessary to align the two scans. Those alignments use standard functionality of the BrainVoyager software.

For each data set, activated voxels were identified by linearly correlating the BOLD signal amplitude with a visual stimulus regressor, formed from a convolution of the visual stimulus time course (set to 1 over the visual stimulation period up to the button press) with a hemodynamic response function (Boynton et al., 1996). The statistical maps were thresholded to the same correlation coefficient of 0.35 for each subject.

Results

Localizing human visual gamma-band activity in time and frequency

Fig. 2 illustrates the overall effect of visual stimulation on the spectral power of sensors overlying visual cortex in one session of subject D. The main effect of visual stimulation was a strong

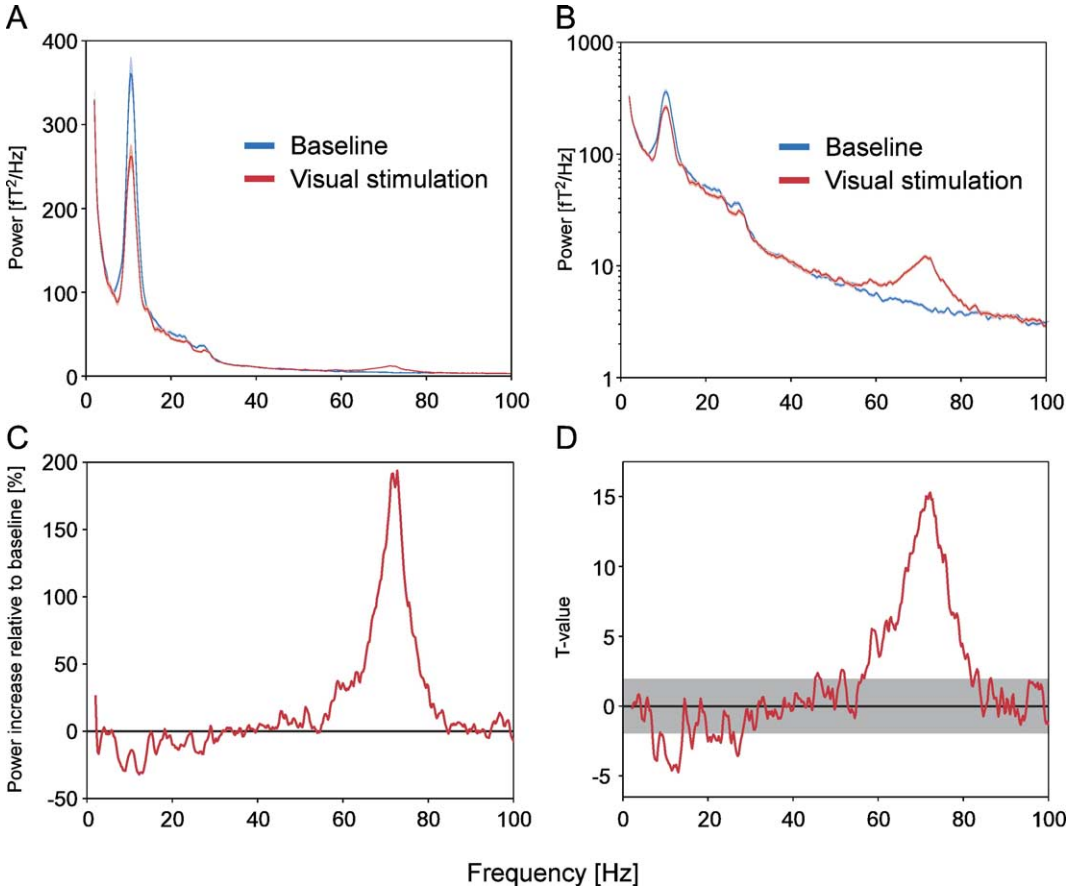

Fig. 2. Visually induced gamma-band activity in one example subject (subject D). (A) Average power spectrum of 28 axial gradiometers overlying visual cortex as a function of frequency, displayed with a linear power-axis. The spectral analysis smoothed the power spectrum with a ±1 Hz rectangular window around each center frequency. (B) The same as panel A but with a logarithmic power axis. (C) The effect of visual stimulation expressed as percent change relative to the baseline. (D) The *t* values for the difference between power during the baseline and during visual stimulation as a function of frequency.

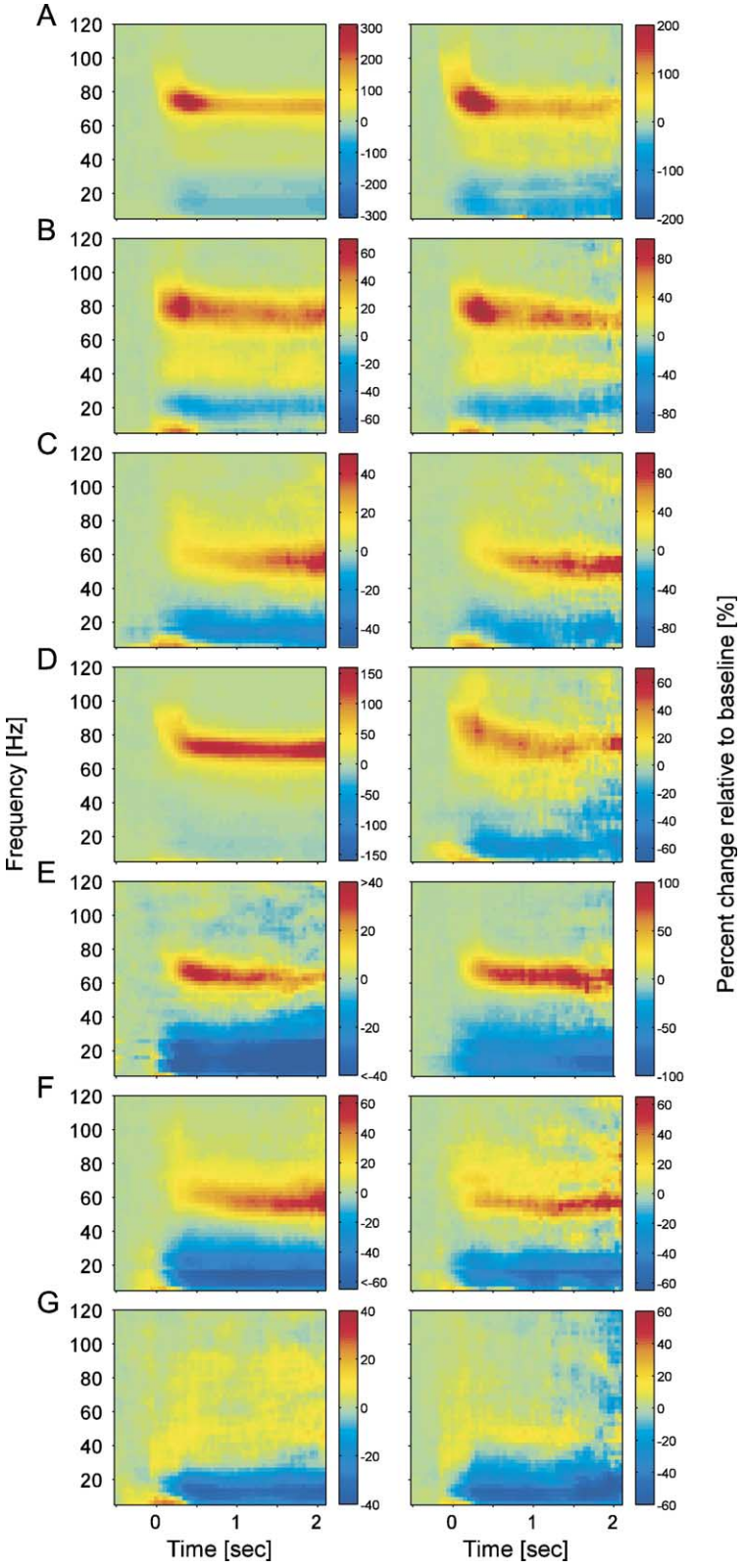

Fig. 3. Time frequency representations of the changes in power in response to visual stimulation. Average of 28 axial gradiometers over visual cortex. Changes are determined relative to the 1-s pre-stimulus baseline. The spectral analysis used here smoothed the power spectrum with a ±5 Hz rectangular window around each center frequency. Rows A through G correspond to subjects A through G. The two columns correspond to the two recordings sessions done per subject. The right panel for subject E is slightly shorter than the others because the respective recording session did not contain a sufficient number of long trials.

increase of power in the gamma band. This can best be seen when power is displayed logarithmically (Fig. 2B). Fig. 2D shows the *t* values for the effect of visual stimulation on power as a function of frequency, illustrating that, in this subject, the visually induced gamma-band activity was the spectral component with the highest signal-to-noise ratio.

We assessed the effect of visual stimulation on MEG power over visual cortex in all seven subjects. Each subject was tested in two recording sessions separated by at least 4 days and by at most 4 months. We found that six out of the seven subjects showed strong gamma-band activity. Figs. 3A–G, representing results from subjects A through G, show the effect of visual stimulation as the percent change in MEG power over visual cortex for both recording sessions. The spectrotemporal pattern of visually induced power changes was quite different for the different subjects but highly replicable across the two recording sessions for all seven subjects. Only the absolute values of the percent changes differed between recordings, and this is most likely explained by differences in head position relative to the sensor helmet that lead to different noise levels for the used sensors over visual cortex.

The percent change spectra in Fig. 3 show several interesting features:

(1) Subject B displayed two clearly discernable peaks in the gamma-frequency range. The lower-frequency peak was around 40 Hz and the higher-frequency peak around 80 Hz. Also subject A showed two separate peaks in the gamma-frequency band, one around 40 and the other around 70 Hz, although this is less appreciable in the color coded time frequency representations.
(2) Subjects C and F showed an increase in gamma-band activity over time.
(3) Subjects A and B showed a transient gamma-band peak around 350 ms after stimulus onset.
(4) We consistently observed that the frequency of the gamma-band peak was somewhat higher at the beginning of the gamma-band response and then settled within about 0.5 s to the frequency that was then sustained. This is similar to other studies in cat, monkey and human (Tallon-Baudry and Bertrand, 1999; Fries et al., 2001, 2002; Rols et al., 2001; Logothetis et al., 2001).

Localizing human visual gamma-band activity in space

Finally, we estimated the locations of the sources of the gamma-band activity. Fig 4 shows the results for subject A. Figs. 4A–G show the effect of visual stimulation on the estimated source power at different frequencies and using different statistics. Figs. 4A–C show the results for estimated source power at 72 ± 8 Hz, that is, the high gamma band. Fig. 4A shows the *t* values obtained after estimating the standard error of the mean for both conditions using a jackknife procedure. Fig. 4B shows the *P* values obtained with a randomization procedure and after correction for the multiple comparisons made across the scanned brain volume. The smallest *P* values that we observed correspond to the maximal significance that can be obtained with the number of randomizations that we used ($P = 1/500$, i.e., $-\log(P) = 2.6990$). Fig. 4C shows the *t* values masked with the *P* values. Fig. 4D shows the same analysis for the second recording session in this subject who was separated from the first session by about 1 month. Source locations were very similar for the two sessions. The absolute *t* values were smaller for the second recording, but this is probably due to a smaller number of trials obtained. Fig. 4E shows the *t* values masked with the *P* values for the estimated source power at 42 ± 3 Hz, that is, the lower gamma-band. Fig. 4F shows the same for 25 ± 5 Hz, that is, the beta-band, and Fig. 4G shows the same for 10 ± 5 Hz, that is, the alpha-band. The power increases in the high and low gamma band showed two peaks confined to the posterior ends of the calcarine sulci of the two hemispheres. This is consistent with sources in the foveal confluence of the early visual areas V1, V2 and V3 (Dougherty et al., 2003). The localizations of power decreases in the alpha- and beta-frequency bands were not as clearly related to the foveal representation.

To get an independent estimate of the brain tissue activated in our paradigm and in this specific subject, we repeated the same experiment (with longer inter-trial intervals) but using functional MRI to image the BOLD signal. The result of this is shown in Fig. 4H. The BOLD signal increases associated with the visual stimulus are closely co-localized with the estimated sources of gamma-band activity. The estimated sources of alpha- and beta-band suppressions were less focal and upon qualitative inspection had only a coarse spatial relation with regions of BOLD signal increases.

The same source analysis was performed for all clear spectral components of the visually induced response of all subjects. The Supplementary material shows all source estimates with significant effects of visual stimulation. Gamma-band activity always localized to a region consistent with the foveal representation.

Discussion

We found human visual gamma-band activity to be a very strong spectral component. While the spectrotemporal pattern of visually induced power changes differed substantially between subjects, it was remarkably constant for a given subject across the two recordings sessions, even if those were separated by as much as 4 months. Inter-subject variability could in principle originate from many different levels. Individual neurons in mammalian cortex exhibit intrinsic oscillatory gamma-band activity upon depolarization (Llinás et al., 1991). Thus, inter-individual variations in basic biophysical parameters like the exact time constants of involved conductances might explain part of the observed differences in the spectral response. Furthermore, the oscillatory characteristics of networks of neurons depend on the network structure and particularly on delays in neuronal interactions (Ermentrout and Kopell, 1998; Kopell et al., 2000). Thus, inter-individual differences could emerge through differences in the functional architecture of early visual areas as described, for example, in the cat visual system (Kaschube et al., 2002). Finally, gamma-band activity is modulated by cognitive factors like attention (Gruber et al., 1999; Fries et al., 2001; Taylor et al., 2005). While the respective studies have so far described changes in the strength of gamma-band activity, it would also be conceivable that cognitive factors change the spectral response pattern. Inter-individual differences might then stem from different amounts of attentional focussing or even different strategies. Given the fairly simple change detection task used in this study and the remarkable constancy of the spectral pattern for a given subject across time, we do not favor this latter possibility.

In some subjects, visually induced gamma-band activity was subdivided into two clearly separate bands. The lower one was around 40 Hz and thus corresponded well with the gamma band

described in several previous EEG studies (Tallon-Baudry et al., 1996). The higher one was between 70 and 80 Hz and thus close to the gamma band described in several MEG studies (Lutzenberger et al., 2002; Kaiser et al., 2003, 2004). A recent study using intracranial EEG showed stimulus induced power enhancements also in two separate gamma-frequency bands roughly correspond-

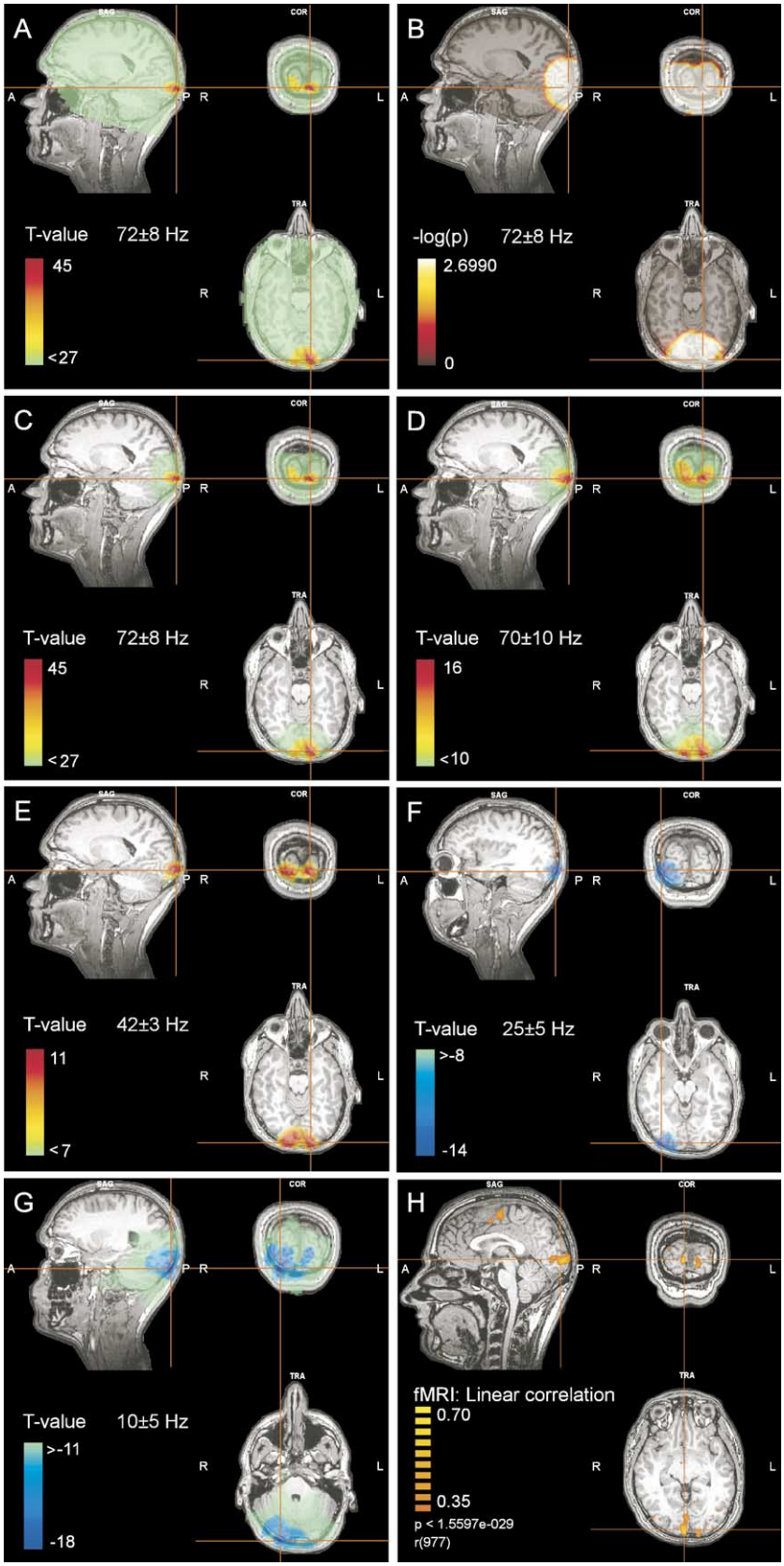

ing to the ones seen here (Tallon-Baudry et al., 2005). We hypothesize that the maximized signal-to-noise ratio in our study allowed us to see both gamma bands simultaneously when they were present.

Irrespective of whether subjects showed one or two gamma bands, a given gamma band was always of limited band width, that is, had a clear lower and upper bound. The underlying neuronal activity was therefore a somewhat regular oscillation. This is in good agreement with many intracortical recordings of gamma-band activity in cats and monkeys (Maldonado et al., 2000; Friedman-Hill et al., 2000; Fries et al., 2001, 2002; Rols et al., 2001; Logothetis et al., 2001; Taylor et al., 2005) but differs from several reports of very broad-band gamma-frequency responses (Tallon-Baudry et al., 2005; Lachaux et al., 2005; Tanji et al., 2005). The studies finding broad-band gamma-frequency responses typically recorded in high-level visual areas and used intracranially recorded EEG from patients with focal epilepsy. Thus, the differences might be due to the different areas recorded or might be related to the medical condition or its treatment.

While the absolute spectral power of the gamma-band activity was very small, it was nevertheless very reliably induced by visual stimulation, resulting in high t values, that is, a high signal-to-noise ratio. Visually induced gamma-band activity was sustained in time as long as visual stimulation and visual processing went on. Adaptive spatial filtering localized the peak of visually induced enhancements of gamma-band activity in all subjects to a cortical region that is consistent with the foveal representation. We cannot infer from this that there was no stimulus induced gamma-band activity in higher visual areas. Future studies, using stimuli that are known to activate higher visual areas, will have to explore this in further detail. In some subjects, we found two spatial peaks of gamma power enhancement in the two hemispheres that might correspond to the two fovea representations. The estimated sources of alpha- and beta-band suppressions were less focal which is in good agreement with other studies (Crone et al., 1998a,b).

Why did this study find strong and reliable visually induced gamma-band activity while many groups find no or substantially less reliable visually induced gamma-band activity with non-invasive methods? This is probably due to a combination of factors.

(1) Paradigms used for investigating stimulus induced changes in spectral power are often still inspired by paradigms used for investigating event related potentials. For the study of event-related potentials, investigators have aimed at obtaining many repetitions of the external event that is used to trigger the averaging of the brain potentials. Thus, trials are short and dominated by the event-related components. This probably reduces the sensitivity for the study of induced gamma-band activity. It has been shown that stimulus induced gamma-band activity in the visual cortex of the cat is inhibited by stimulus transients and the corresponding response transients (Kruse and Eckhorn, 1996). In order to optimize the conditions for investigating stimulus induced gamma-band activity, we used visual stimulation that lasted for up to 3 s and did not contain stimulus transients.

(2) Many previous studies have investigated the stimulus dependence of visual gamma-band activity in animals and humans (Gray et al., 1989; Tallon-Baudry et al., 1996; Gail et al., 2000). The general finding is that gamma-band activity is found most strongly and reliably for coherent stimuli and in particular for coherently moving stimuli. This might be related to stronger neuronal activation with moving stimuli and we therefore used a concentric sine wave grating that contracted smoothly towards the fixation point.

(3) Our stimulus was presented in the fovea. In the human, the fovea is represented by a large part of visual cortex. Furthermore, the foveal representation is closer to the surface than the representation of the visual periphery. Both, the large number of neurons involved and their superficial location have probably contributed to the strength of the observed gamma-band activity.

(4) We optimized the stimulus to activate a large number of neurons in the foveal representation, that is, the stimulus was large, had a high contrast, had an optimal spatial frequency and was slowly moving (see Materials and methods for the detailed stimulus specification).

(5) It has been shown that visual attention enhances stimulus induced gamma-band activity in monkey and human visual cortex (Gruber et al., 1999; Fries et al., 2001). We therefore had subjects report a stimulus change that could occur at an unpredictable moment in time after stimulus onset (Fries et al., 2001). This made them monitor the stimulus attentively for the entire duration of the stimulus presentation.

(6) The gamma band is often about 20 Hz wide, that is, much wider than, for example, the typical alpha band or the typical beta band. It is therefore important to perform an appropriate spectral concentration. We achieved this by using multi-taper spectral analysis techniques (Mitra and Pesaran, 1999; Jarvis and Mitra, 2001; Pesaran et al., 2002). For the gamma-band activity, we typically used multiple tapers that lead to a boxcar smoothing of the spectrum with a box width of 20 Hz. The power estimate at 50 Hz is thus the average power between 40 and 60 Hz. The effect of this spectral concentration is particularly pronounced when the analysis window is long, which would normally result in a high spectral resolution. Concentrating over a relatively broad spectral band will in this case be equivalent to averaging over many spectral bins and thereby lead to a substantial reduction in variance. For the source analysis, we have concentrated spectral energy maximally by adjusting the multi-tapers to each individual band of each recording session. This was one factor contributing to the high t values on the source level (e.g., Fig. 4A).

(7) We used adaptive spatial filtering to estimate the sources of oscillatory signals. Those spatial filters combine signals from

Fig. 4. MEG source analysis and fMRI BOLD contrast for subject A. (A) The t values for the difference in estimated source power at 72 ± 8 Hz between baseline and visual stimulation. The threshold of the color axis was raised to 60% of the maximal absolute t value in order to resolve the fine spatial structure around the peaks. This holds also for the other panels showing t values. (B) Same as panel A, but displaying P values obtained with the randomization procedure including a correction for multiple comparisons. (C) The t values from panel A, but masked with the P values from panel B. (D) The same as panel C, but for the second recording session in this subject and for 70 ± 10 Hz. Panels E, F and G show the same analysis as panel C, but for different frequency bands as indicated on those panels. (H) The correlation of the fMRI BOLD response with the visual stimulus regressor. The structural MRIs used for the coregistration with the MEG data and for the coregistration with the fMRI data are from the same subject, but from two different MRI sessions.

multiple sensors and thereby also enhance the signal-to-noise ratio.

(8) It has been argued that low amplitude signals can best be detected with a measurement device with high amplitude resolution (Lutzenberger et al., 2002; Kaiser et al., 2003, 2004). MEG systems differ in that respect. We used the same system as Lutzenberger et al. (2002) and Kaiser et al. (2003, 2004).

While all those points have likely contributed to increasing the sensitivity, no single one appears to be a *conditio sine qua non*. Gamma-band activity has been described for short stimulus durations (Rols et al., 2001; Tallon-Baudry et al., 2001), stationary stimuli (Rols et al., 2001) and in the absence of focused attention (Maldonado et al., 2000; Friedman-Hill et al., 2000). Also, optimized spectral concentration was not an absolute pre-requisite as the analysis in Fig. 2 shows clear gamma-band activity with very limited spectral concentration (±1 Hz rectangular windows around each center frequency).

We conclude that with optimal stimulation, behavioral paradigm, measurement equipment and data analysis, human visual gamma-band activity can be studied with a very high signal-to-noise ratio and that it can be accurately localized in frequency, time and space. This will provide an important window onto human visual gamma-band activity that will allow us to investigate its functional role in future studies.

Acknowledgments

We thank O. Jensen, P. Mitra and D. Norris for helpful discussions and suggestions. Supported by The Netherlands Organization for Scientific Research, grants 452-03-344 and 051-02-050 (P.F.), The Human Frontier Science Program Organization, grant RGP0070/2003 (P.F.), and the Danish Technical Research Council, grant 26-01-0092 (R.O.).

Appendix A. Supplementary data

Supplementary data associated with this article can be found in the online version at doi:10.1016/j.neuroimage.2005.08.043.

References

Adjamian, P., Holliday, I.E., Barnes, G.R., Hillebrand, A., Hadjipapas, A., Singh, K.D., 2004. Induced visual illusions and gamma oscillations in human primary visual cortex. Eur. J. Neurosci. 20, 587–592.

Boynton, G.M., Engel, S.A., Glover, G.H., Heeger, D.J., 1996. Linear systems analysis of functional magnetic resonance imaging in human V1. J. Neurosci. 16, 4207–4221.

Bressler, S.L., Coppola, R., Nakamura, R., 1993. Episodic multiregional cortical coherence at multiple frequencies during visual task performance. Nature 366, 153–156.

Crone, N.E., Miglioretti, D.L., Gordon, B., Lesser, R.P., 1998a. Functional mapping of human sensorimotor cortex with electrocorticographic spectral analysis: II. Event-related synchronization in the gamma band. Brain 121 (Pt. 12), 2301–2315.

Crone, N.E., Miglioretti, D.L., Gordon, B., Sieracki, J.M., Wilson, M.T., Uematsu, S., Lesser, R.P., 1998b. Functional mapping of human sensorimotor cortex with electrocorticographic spectral analysis: I. Alpha and beta event-related desynchronization. Brain 121 (Pt. 12), 2271–2299.

Dougherty, R.F., Koch, V.M., Brewer, A.A., Fischer, B., Modersitzki, J., Wandell, B.A., 2003. Visual field representations and locations of visual areas V1/2/3 in human visual cortex. J. Vis. 3, 586–598.

Eckhorn, R., Bauer, R., Jordan, W., Brosch, M., Kruse, W., Munk, M., Reitboeck, H.J., 1988. Coherent oscillations: a mechanism of feature linking in the visual cortex? Multiple electrode and correlation analyses in the cat. Biol. Cybern. 60, 121–130.

Efron, B., Tibshirani, R.J., 1993. An Introduction to the Bootstrap. Chapman & Hall/CRC.

Engel, A.K., König, P., Singer, W., 1991. Direct physiological evidence for scene segmentation by temporal coding. Proc. Natl. Acad. Sci. U. S. A. 88, 9136–9140.

Ermentrout, G.B., Kopell, N., 1998. Fine structure of neural spiking and synchronization in the presence of conduction delays. Proc. Natl. Acad. Sci. U. S. A. 95, 1259–1264.

Friedman-Hill, S., Maldonado, P.E., Gray, C.M., 2000. Dynamics of striate cortical activity in the alert macaque: I. Incidence and stimulus-dependence of gamma-band neuronal oscillations. Cereb. Cortex 10, 1105–1116.

Fries, P., Reynolds, J.H., Rorie, A.E., Desimone, R., 2001. Modulation of oscillatory neuronal synchronization by selective visual attention. Science 291, 1560–1563.

Fries, P., Schröder, J.H., Roelfsema, P.R., Singer, W., Engel, A.K., 2002. Oscillatory neuronal synchronization in primary visual cortex as a correlate of stimulus selection. J. Neurosci. 22, 3739–3754.

Gail, A., Brinksmeyer, H.J., Eckhorn, R., 2000. Contour decouples gamma activity across texture representation in monkey striate cortex. Cereb. Cortex 10, 840–850.

Gray, C.M., Singer, W., 1989. Stimulus-specific neuronal oscillations in orientation columns of cat visual cortex. Proc. Natl. Acad. Sci. U. S. A. 86, 1698–1702.

Gray, C.M., König, P., Engel, A.K., Singer, W., 1989. Oscillatory responses in cat visual cortex exhibit inter-columnar synchronization which reflects global stimulus properties. Nature 338, 334–337.

Gray, C.M., Engel, A.K., König, P., Singer, W., 1992. Synchronization of oscillatory neuronal responses in cat striate cortex: temporal properties. Vis. Neurosci. 8, 337–347.

Gross, J., Kujala, J., Hamalainen, M., Timmermann, L., Schnitzler, A., Salmelin, R., 2001. Dynamic imaging of coherent sources: studying neural interactions in the human brain. Proc. Natl. Acad. Sci. U. S. A. 98, 694–699.

Gruber, T., Müller, M.M., Keil, A., Elbert, T., 1999. Selective visual-spatial attention alters induced gamma band responses in the human, EEG. Clin. Neurophysiol. 110, 2074–2085.

Gruber, T., Keil, A., Müller, M.M., 2001. Modulation of induced gamma band responses and phase synchrony in a paired associate learning task in the human EEG. Neurosci. Lett. 316, 29–32.

Jarvis, M.R., Mitra, P.P., 2001. Sampling properties of the spectrum and coherency of sequences of action potentials. Neural Comput. 13, 717–749.

Kaiser, J., Ripper, B., Birbaumer, N., Lutzenberger, W., 2003. Dynamics of gamma-band activity in human magnetoencephalogram during auditory pattern working memory. NeuroImage. 20, 816–827.

Kaiser, J., Bühler, M., Lutzenberger, W., 2004. Magnetoencephalographic gamma-band responses to illusory triangles in humans. NeuroImage 23, 551–560.

Kaschube, M., Wolf, F., Geisel, T., Löwel, S., 2002. Genetic influence on quantitative features of neocortical architecture. J. Neurosci. 22, 7206–7217.

Keil, A., Müller, M.M., Ray, W.J., Gruber, T., Elbert, T., 1999. Human gamma band activity and perception of a gestalt. J. Neurosci. 19, 7152–7161.

Kopell, N., Ermentrout, G.B., Whittington, M.A., Traub, R.D., 2000. Gamma rhythms and beta rhythms have different synchronization properties. Proc. Natl. Acad. Sci. U. S. A. 97, 1867–1872.

Kreiter, A.K., Singer, W., 1996. Stimulus-dependent synchronization of neuronal responses in the visual cortex of the awake macaque monkey. J. Neurosci. 16, 2381–2396.

Kruse, W., Eckhorn, R., 1996. Inhibition of sustained gamma oscillations (35–80 Hz) by fast transient responses in cat visual cortex. Proc. Natl. Acad. Sci. U. S. A. 93, 6112–6117.

Lachaux, J.P., George, N., Tallon-Baudry, C., Martinerie, J., Hugueville, L., Minotti, L., Kahane, P., Renault, B., 2005. The many faces of the gamma band response to complex visual stimuli. NeuroImage 25, 491–501.

Llinás, R.R., Grace, A.A., Yarom, Y., 1991. In vitro neurons in mammalian cortical layer 4 exhibit intrinsic oscillatory activity in the 10- to 50-Hz frequency range. Proc. Natl. Acad. Sci. U. S. A. 88, 897–901.

Logothetis, N.K., Pauls, J., Augath, M., Trinath, T., Oeltermann, A., 2001. Neurophysiological investigation of the basis of the fMRI signal. Nature 412, 150–157.

Lutzenberger, W., Ripper, B., Busse, L., Birbaumer, N., Kaiser, J., 2002. Dynamics of gamma-band activity during an audiospatial working memory task in humans. J. Neurosci. 22, 5630–5638.

Maldonado, P.E., Friedman-Hill, S., Gray, C.M., 2000. Dynamics of striate cortical activity in the alert macaque: II. Fast time scale synchronization. Cereb. Cortex 10, 1117–1131.

Miltner, W.H., Braun, C., Arnold, M., Witte, H., Taub, E., 1999. Coherence of gamma-band EEG activity as a basis for associative learning. Nature 397, 434–436.

Mima, T., Oluwatimilehin, T., Hiraoka, T., Hallett, M., 2001. Transient interhemispheric neuronal synchrony correlates with object recognition. J. Neurosci. 21, 3942–3948.

Mitra, P.P., Pesaran, B., 1999. Analysis of dynamic brain imaging data. Biophys. J. 76, 691–708.

Nichols, T.E., Holmes, A.P., 2001. Nonparametric permutation tests for functional neuroimaging: a primer with examples. Hum. Brain Mapp. 15, 1–25.

Pesaran, B., Pezaris, J.S., Sahani, M., Mitra, P.P., Andersen, R.A., 2002. Temporal structure in neuronal activity during working memory in macaque parietal cortex. Nat. Neurosci. 5, 805–811.

Press, W.H., Flannery, B.P., Teukolsky, S.A., 1992. Numerical Recipes in C. Cambridge Univ. Press, Cambridge.

Rodriguez, E., George, N., Lachaux, J.P., Martinerie, J., Renault, B., Varela, F.J., 1999. Perception's shadow: long-distance synchronization of human brain activity. Nature 397, 430–433.

Roelfsema, P.R., Engel, A.K., König, P., Singer, W., 1997. Visuomotor integration is associated with zero time-lag synchronization among cortical areas. Nature 385, 157–161.

Rols, G., Tallon-Baudry, C., Girard, P., Bertrand, O., Bullier, J., 2001. Cortical mapping of gamma oscillations in areas V1 and V4 of the macaque monkey. Vis. Neurosci. 18, 527–540.

Steinmetz, P.N., Roy, A., Fitzgerald, P.J., Hsiao, S.S., Johnson, K.O., Niebur, E., 2000. Attention modulates synchronized neuronal firing in primate somatosensory cortex. Nature 404, 187–190.

Tallon-Baudry, C., Bertrand, O., 1999. Oscillatory gamma activity in humans and its role in object representation. Trends Cogn. Sci. 3, 151–162.

Tallon-Baudry, C., Bertrand, O., Delpuech, C., Pernier, J., 1996. Stimulus specificity of phase-locked and non-phase-locked 40 Hz visual responses in human. J. Neurosci. 16, 4240–4249.

Tallon-Baudry, C., Bertrand, O., Delpuech, C., Permier, J., 1997a. Oscillatory gamma-band (30–70 Hz) activity induced by a visual search task in humans. J. Neurosci. 17, 722–734.

Tallon-Baudry, C., Bertrand, O., Wienbruch, C., Ross, B., Pantev, C., 1997b. Combined EEG and MEG recordings of visual 40 Hz responses to illusory triangles in human. NeuroReport 8, 1103–1107.

Tallon-Baudry, C., Bertrand, O., Peronnet, F., Pernier, J., 1998. Induced gamma-band activity during the delay of a visual short-term memory task in humans. J. Neurosci. 18, 4244–4254.

Tallon-Baudry, C., Bertrand, O., Fischer, C., 2001. Oscillatory synchrony between human extrastriate areas during visual short-term memory maintenance. J. Neurosci. 21, RC177.

Tallon-Baudry, C., Bertrand, O., Hénaff, M.A., Isnard, J., Fischer, C., 2005. Attention modulates gamma-band oscillations differently in the human lateral occipital cortex and fusiform gyrus. Cereb. Cortex 15, 654–662.

Tanji, K., Suzuki, K., Delorme, A., Shamoto, H., Nakasato, N., 2005. High-frequency gamma-band activity in the basal temporal cortex during picture-naming and lexical-decision tasks. J. Neurosci. 25, 3287–3293.

Taylor, K., Mandon, S., Freiwald, W.A., Kreiter, A.K., 2005. Coherent oscillatory activity in monkey area V4 predicts successful allocation of attention. Cereb. Cortex 15, 1424–1437.